Journal of Control, Automation and Electrical Systems (2019) 30:27–40
https://doi.org/10.1007/s40313-018-00424-z

A Novel Approach for Stall Prevention and Rotation Speed Limiting in a Min–Max Controller Structure

Antonio Hadade Neto[1] · **Takashi Yoneyama**[1]

Received: 20 March 2018 / Revised: 4 September 2018 / Accepted: 11 October 2018 / Published online: 5 November 2018

Abstract
This paper proposes a novel approach for the implementation of limit controllers used for stall prevention and rotation speed limitation of a single-spool jet engine. In this approach, the protection requirements regarding the rotation speed are achieved through the use of a filter applied to the reference that will be sent to the power management controller of a Min–Max structure controller. The main controller variable is the turbine's core rotation speed. The filter chooses the most appropriate reference value aiming at respecting the engine established limits, such as the stall margin and the maximum rotation speed, during transient and steady-state behaviors. The Min–Max compensators structure chosen for the implementation of the controllers is proportional–integral with Back Calculation as the anti-windup technique. Simulation model of a GE-J85-13 single-spool jet engine has been used to test the new approach and compare it to the more common Min–Max structure, where each controller is implemented individually. The simulation contemplates the case where a step function is applied to the power management controller, where the final value is the maximum allowed rotation speed value, at sea-level, static and standard-day temperature conditions. The simulation is repeated for different values of Back Calculation gains using both Min–Max structures, and the behavior of the GE-J85-13 engine is evaluated in each case for comparison proposes.

Keywords Jet engine · Stall prevention · Min–Max · Proportional–integral · Speed limitation · Back Calculation · Windup · Reference filter

List of Symbols

$\mathrm{AS}(N_c)$	Acceleration schedule vector
$\mathrm{AS}_{N_c}^{\mathrm{Vec}}$	Acceleration schedule vector containing the maximum allowed variations for given values of N_c
e	Process error
e_{I}	Integrator error
EPR	Engine pressure ratio
e_{ss}	Steady value of PI compensator error
F_{n}	Net thrust
$\mathrm{FR_N}$	Rotation speed filtered reference
I	Moment of inertia of the engine's rotating set
K_{b}	Back Calculation constant
K_{bN}	Back Calculation constant used on a rotation speed controller
K_{bT}	Back Calculation constant used on a temperature controller
K_{i}	Integrator term constant of a PI compensator
K_{p}	Proportional term constant of a PI compensator
N	Shaft mechanical rotation speed
N_{c}	Shaft corrected rotation speed
N_{D}	Design point rotation speed
N_{max}	Maximum allowed mechanical rotation speed
N_c^{Vec}	Vector containing N_c values and used in acceleration schedule
PI	Proportional–integral compensator
P_{s3}	Combustion chamber static pressure
P_{t2}	Compressor inlet total pressure
P_{t5}	Turbine inlet total pressure
PR	Compressor pressure ratio
$\mathrm{PR_{stall}}$	Compressor pressure ratio for stall occurrence at a given N_c
$\mathrm{Ref_N}$	Rotation speed desired reference

✉ Antonio Hadade Neto
antonio.hadade@gmail.com

[1] Praça Marechal Eduardo Gomes, 50 - Vila das Acácias, São José dos Campos, SP, Brazil

RU	Ratio unit parameter
RU_{min}	Minimum value allowed for RU parameter
SM	Stall margin
t_s	Settling time
T_s	Sample Period
T_{t2}	Compressor inlet total temperature
T_{t4}	Turbine inlet temperature
T_{t4max}	Maximum allowed TIT
T_{t5}	Turbine exhaust temperature
T_{std}	Standard-day temperature
u	Actuation signal calculated by PI compensator
u_{0a}	Initial steady value of actuation signal calculated by acceleration limit controller
$u_{0T_{t4}}$	Initial steady value of actuation signal calculated by T_{t4} limit controller;
u_{0N}	Initial steady value of actuation signal calculated by N limit controller
u_{0pm}	Initial steady value of actuation signal calculated by power management controller
u_{0r}	Initial steady value of real actuation signal
u_{min}	Minimum allowed actuation signal
u_{max}	Maximum allowed actuation signal
u_{ss}	Steady value of actuation signal calculated by PI compensator
u_r	Actual control signal sent to engine's fuel pump
u_{rss}	Real actuation signal steady value
W_c	Power demanded by the jet engine's compressor
w_f	Fuel mass flow
W_t	Power delivered by the jet engine's turbine

1 Introduction

A single-spool jet engine is an approximate practical implementation of the Joule–Brayton thermodynamic cycle (Richter 2012a), being its basic functioning described as follows: air enters the compressor, where a compression process occurs, increasing the air total pressure and temperature. Following, the compressed air enters a combustion chamber, where fuel is injected and burned at constant pressure, increasing the working gas temperature. Next, an expansion process is accomplished at the turbine and energy is extracted from the gas to be provided directly to the compressor through the mechanical coupling between those two components. Finally, the exhausting gas from the turbine is accelerated by a nozzle with the remaining energy present in the gas converted into the desired thrust. Figure 1 shows a basic diagram of a single-spool jet engine, which corresponds to the configuration of the GE J85-13 jet engine (no afterburner), whose mathematical model has been implemented with the use of T-MATS simulation tool (Chappman et al. 2014) for the accomplishment of this work.

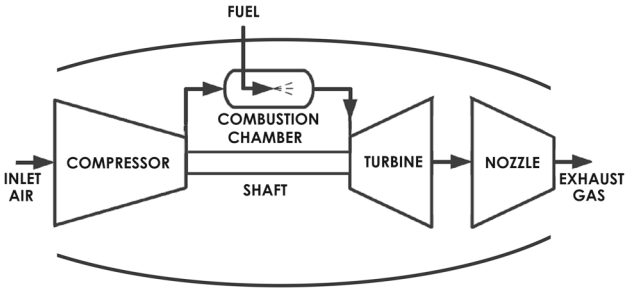

Fig. 1 Basic diagram of a single-spool jet engine

The jet engine control problem consists of providing the desired level of thrust with minimum steady error while presenting a transient regime which should be fast enough for the aircraft to be able to accomplish the required maneuvers. Furthermore, the controller must avoid undesired situations during operation, such as compressor stall (Jaw and Mattingly 2009), over temperature or combustion chamber blow out.

Min–Max structure with linear actuators is a control strategy widely used in commercial engines since the 1970's (Imani and Montazeri-Gh 2017). In this technique, each engine limit and a main controlled variable (typically rotation speed) are treated by individual controllers and the control signal considered to be the most appropriate is selected aiming to preserve safety operation while granting transient and steady-state requirements.

Compressor stall avoidance (Csank et al. 2010) in a jet engine is extremely important, since the stall phenomena (characterized by the loss of capability by the compressor of compressing the working fluid, as explained with more details in Jaw and Mattingly (2009), may cause catastrophic accidents. It is also desired that no significant performance loss occurs while avoiding stall. Csank et al. (2010) and Jaw and Mattingly (2009) have presented methods for stall avoidance on turbofan engines using direct acceleration control in a Min–Max structure with PI compensators and Back Calculation as anti-windup protection. In those methods, a separate compensator for direct control of acceleration is used and the maximum allowed acceleration is a function of the normalized core rotation speed.

This work proposes a novel method for stall avoidance where engine acceleration is controlled through the appliance of a reference filter to the input of a compensator identical to the one used to control the engine's rotation speed—the main controlled variable. The Min–Max structure and the PI compensators with Back Calculation are maintained. For the effect of comparison, simulations of the rotation speed and acceleration being controlled separately, as suggested by literature (Csank et al. 2010; Jaw and Mattingly 2009), and

appliance of the reference filter directly to the rotation speed compensator have been carried out. It is shown that the use of the reference filter directly on the rotation speed reference results in a simpler controller with less sensitiveness to Back Calculation gain variation.

2 The Min–Max Control Structure

This section provides a brief explanation of the Min–Max control structure, commonly used in commercial jet engines and suitable for single-spool engines as well (detailed explanations of the concepts addressed in this section are found in Richter (2012b), Csank et al. (2010) and Jaw and Mattingly (2009). For illustrative purposes, a generic block diagram of the Min–Max structure with a total of four variables is shown in Fig. 2. The controlled variables are V_0, V_1, V_2 and V_3, where V_0 represents the main variable to be controlled by the power management controller and the remaining ones are controlled by the limit controllers (maximum and minimum limits). In the case of a single-spool jet engine, the main variable V_0 is the rotation speed and the variables V_i for $i \neq 0$ are parameters having a maximum limit, such as T_{t4} or minimum limit, such as RU. Ref_0 represents the desired value for V_0; E_0 is the power management controller error, given by $\mathrm{Ref}_0 - V_0$, being C_0 the compensator generating the control signal responsible for driving the output V_0 to Ref_0. Each limit controller variables V_i, where $i = 1, 2, 3$, also have its respective individual compensator C_i. $\mathrm{Ref}_{i\mathrm{Max}}$ represents the maximum value allowed for the variable V_i and $\mathrm{Ref}_{i\mathrm{Min}}$ the minimum value allowed for the variable V_i. The errors $E_{i\mathrm{Max}} = \mathrm{Ref}_{i\mathrm{Max}} - V_i$ and $E_{i\mathrm{Min}} = \mathrm{Ref}_{i\mathrm{Min}} - V_i$ are the errors referred to the maximum and minimum values of V_i. It should be noticed that the objective of the actuation signal generated by each compensator C_i is to drive the variable V_i to its established limits, $\mathrm{Ref}_{i\mathrm{Max}}$ or $\mathrm{Ref}_{i\mathrm{Min}}$. The compensators gains, which are inputs of C_0 and C_i, may change their values to take into account any nonlinearity inherent to the controlled system. Therefore, gain scheduling may become necessary and is accomplished by the *Schedule* block, whose outputs, the gains for each compensator, are functions of its inputs, the main variable V_0 and the ambient conditions, given by *Altitude* and *FlightSpeed* blocks.

The actuation signal generated by the power management controller C_0 and the signal generated by the various maximum limit controllers, i.e., C_i compensators having $E_{i\mathrm{Max}}$ as inputs, are passed through the Min block which selects the lowest input and sets it as output. Then, the output from the Min block and the signals generated by the various minimum limit controllers, i.e., compensators having $E_{i\mathrm{Min}}$ as inputs, are passed through the Max block, which works similarly to the Min block, but selecting the largest input value as output. Finally, the Max block output is sent to the engines fuel pump.

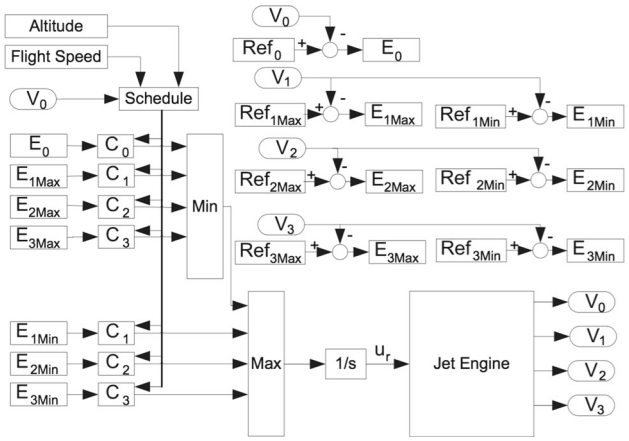

Fig. 2 Block diagram of Min–Max configuration

In the commonly used Min–Max structure, the power management controller and the limit controllers are normally separated, so that each corresponding variable is managed by an individual compensator. The purpose of the integrator at the final output is to attain absence of steady-state error for the main variable. It is important to notice that, not necessarily, a variable V_i used to guarantee both the maximum and a minimum limit, as shown in Fig. 2. Depending on the design requirements, a variable V_i might be used to control exclusively a minimum or a maximum limit (Csank et al. 2010).

3 GE-J85-13 Jet Engine Model

A nonlinear model of a GE J85-13 jet engine (no afterburner) has been implemented and used in this work for performing the simulations necessary to analyze the novel proposed control scheme. For the implementation, T-MATS (Chappman et al. 2014), a Simulink® toolbox designed for simulating thermodynamic systems which describes the engine in terms components individual blocks, has been used. The corresponding block diagram is shown in Fig. 3.

For a more complete and accurate model of GE J85-13 to be obtained, both the engine compressor and turbine must be described in terms of component maps. Data for building compressor and turbine maps, and performance data are found in Chapman et al. (2016), Kopasakis et al. (2010) and Yarlagadda (2010).

Component blocks are described as follows: an ambient block, which calculates the inlet engine conditions based on the altitude and the flight Mach number, a compressor block, which relies on the compressor map to calculate the compressor outputs and the consumed power, a combustion

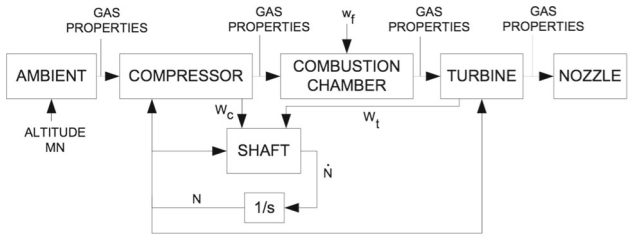

Fig. 3 Block diagram of GE-J85-13 jet engine

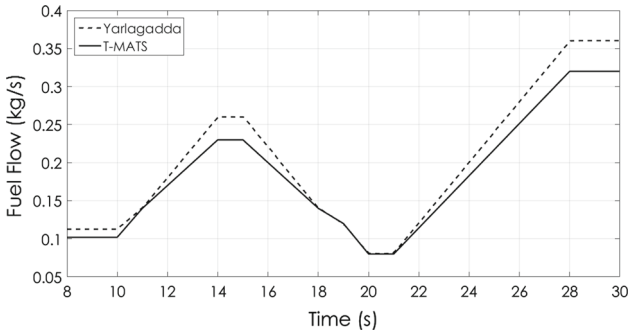

Fig. 4 Comparison of fuel flow w_f obtained by Yarlagadda (2010) with the ones obtained by the author's model

chamber block, which calculates the turbine inlet temperature conditions based on the amount of fuel flow, turbine block, which calculates the turbine's exhaust conditions as well as the delivered power, exhaust nozzle block, which calculates the thrust and the exhaust gas conditions, and a shaft block, which uses the difference between turbine and compressor power together with the current rotation speed to represent the shaft dynamics. T-MATS uses a very complete and complex set of thermodynamic relations, and for balancing all equations, interaction algorithms, such as Newton–Raphson, are used.

For control design purposes, it is enough that only the shaft dynamics is considered (Kopasakis et al. 2010). Therefore, T-MATS model does not take into account volume dynamics and the only differential equation used in the model is the one describing rotation speed variation (shaft block) and given by the equation below:

$$\frac{2\pi}{60}\frac{\mathrm{d}}{\mathrm{d}t}N = \frac{1}{I}(W_\mathrm{t} - W_\mathrm{c}) \tag{1}$$

In Yarlagadda (2010), an alternative modeling technique is presented where volume dynamics is considered, resulting in a more complex model then the one implemented in T-MATS. A comparison between open loop dynamic behavior obtained from simulations of both models is shown in Figs. 4 and 5 where the curves of fuel flow w_f and net thrust F_n are exhibited. It can be noticed that a good match is achieved, with minor differences due to slightly different design point specification in each case.

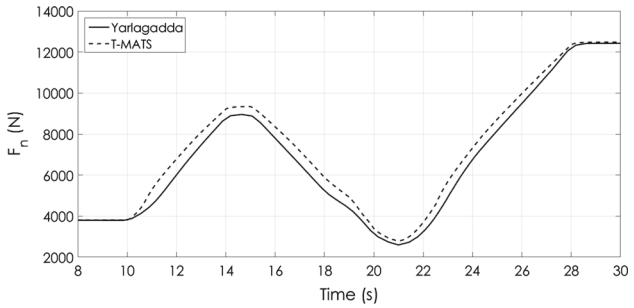

Fig. 5 Comparison of net thrust F_n obtained by Yarlagadda (2010) with the ones obtained by the author's model

4 Selection of Min–Max Linear: PI Compensator Structure

For a better analysis of the engine dynamics and easier design of the Min–Max linear compensators, a set of operating points have been chosen where small perturbations have been applied to the actuation signal and state variable in order for the corresponding state-space matrices to be obtained at each operating point. Since only the shaft dynamics is considered, the linear models obtained for the main controlled variable and the limited variables are of first order and share the same pole. The state-space model obtained is shown by the system of equations (2), where the indexes i and j indicate, respectively, the ith operating point and the jth variable y_j for which the state-space coefficients a_i, b_i, c_{ij} and d_{ij} have been obtained. Considering that the index $j = 0$ represents the main controlled variable, i.e., $y_0 = N$, it is straightforward that $c_{i0} = 1$ and $d_{i0} = 0$.

$$\begin{cases} \dfrac{\mathrm{d}}{\mathrm{d}t}N = a_i N + b_i w_\mathrm{f} \\ \quad y_j = c_{ij} N + d_{ij} w_\mathrm{f} \end{cases} \tag{2}$$

Applying the Laplace transform to the state-spate equations (2) and considering the Laplace transforms $\mathscr{L}\{y_i\} = Y_i(s)$, $\mathscr{L}\{N\} = N(s)$ and $\mathscr{L}\{w_\mathrm{f}\} = W_\mathrm{f}(s)$, local transfer functions $G_{ij}(s)$ are obtained and described by Eq. (3):

$$G_{ij}(s) = \frac{Y_j(s)}{W_\mathrm{f}(s)} = \frac{d_{ij}s + (c_{ij}b_i - d_{ij}a_i)}{s - a_i} \tag{3}$$

In the case of the main controlled variable N, an individual compensator has been designed for each different transfer function and gain scheduling with linear interpolation has been used for choosing the controller gains as a function of the measured value of N during engine operation. Chapman and Litt (2017) and Csank et al. (2010) suggest that no gain scheduling is used in the case of the limited variables, which has been respected in this work. Therefore, for the limited variables, only the transfer function obtained at the

points where the respective limit values occur has been considered, resulting in asymptotically stable minimum phase first order plants in all situations, where $c_{ij} < 0$ and $d_{ij} > 0$ if y_i corresponds to a temperature variable, such as T_{t4}, and $c_{ij} > 0$ and $d_{ij} > 0$ if y_i corresponds to a pressure variable, such as P_{s3}, and $a_i < 0$ and $b_i > 0$ in any case. The PI structure has been chosen in this work for its known good performance and simplicity of tuning in the analyzed cases and for its large acceptance within aeronautical industry. Csank et al. (2010), Jaw and Mattingly (2009) and Chapman and Litt (2017) also adopt PI structure due to its good performance and acceptance in their proposed methods. For a digital implementation of the PI compensator, the forward Euler discretization method has been chosen, where the error signal is delayed by a sample period unit before it is integrated.

5 Anti-Windup Method: Back Calculation

The integrator windup phenomena occurs when the nominal control u calculated and commanded by the PI is not achieved due to actuator limitations, with $u \neq u_r$, where u_r is the real actuating signal sent to the controlled system (Hodel and Hall 2001). Typically, a large value is observed at the integrator output. This phenomenon is likely to happen in the Min–Max structure using PI compensators, since, at steady-state regime, only one of the compensators is actually active, having its calculated signal sent to the controlled plant, while the integrators present on remaining compensators will increase their respective control signals indefinitely, since the corresponding errors are normally not zero. This may lead inactive controllers never to be activated again due to the Min–Max logic.

Many techniques have been implemented for avoiding the windup phenomena. Among the most commonly used, Back Calculation (Visioli 2003), also adopted in Csank et al. (2010) and Chapman and Litt (2017), is the one chosen for this work. The technique consists of adding a term to the integral error e_I of the PI as shown by the equation below:

$$e_I = e - K_b(u - u_r) \tag{4}$$

The extra term considers the difference between the real actuating signal u_r and the signal u calculated by the PI compensator. The constant K_b determines the rate at which the integral term is reset (Visioli 2003) and plays direct influence on the controllers performance.

The Back Calculation technique diminishes the error seen by the integrator and brings its output to a suitable steady value whenever the controller is not active. This characteristic keeps the correspondent controller from not being ever selected by the Min–Max structure and reduces the size of an instantaneous change in magnitude of the control signal when the controller becomes active (Csank et al. 2010).

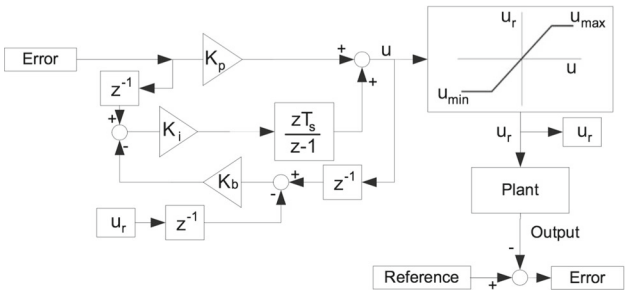

Fig. 6 Block diagram of PI structure with Back Calculation anti-windup method

Figure 6 shows the block diagram of the PI compensator using Back Calculation as anti-windup technique. The block *Error* has, as an output, the difference between the reference (*Reference* block) and the measured controlled variable (*Output* parameter of the *Plant* block). The parameters K_p and K_i are, respectively, the proportional and integral gains and K_b is the Back Calculation gain, which must be carefully chosen for proper functioning of the adopted method. The parameters u_{min} and u_{max} are, respectively, the minimum and maximum values allowed for the real actuation signal u_r, where:

$$\begin{aligned} u_r &= u \; if \; u_{min} \leq u \leq u_{max} \\ u_r &= u_{min} \; if \; u < u_{min} \\ u_r &= u_{max} \; if \; u > u_{max} \end{aligned} \tag{5}$$

In the case of study approached in this work, the values u_{max} and u_{min} are determined by the Min–Max structure control logic in its attempt to respect the established engine limits during operation.

Following, a short analysis of the Back Calculation technique stability and the conditions that must be respected during the choice of K_b are obtained. The digital control law for the PI with Back Calculation, in terms of Z-Transform, is given by Eq. (6). Considering Z-Transforms of the error signal, the actuation signal calculated by the PI compensator, u, and the real control signal sent to system to be controlled, u_r, denote, respectively, by $E(z)$, U_z and $U_r(z)$, one has that:

$$\begin{aligned} U(z) = K_p E(z) + K_i z^{-1} E(z) \frac{zT_s}{z-1} \\ - K_i T_s K_b \left[z^{-1} U(z) - z^{-1} U_r(z) \right] \frac{zT_s}{z-1} \end{aligned} \tag{6}$$

Rearranging Eq. (6), one gets:

$$\begin{aligned} (z-1)U(z) = (z-1)K_p E(z) + K_i T_s E(z) \\ - K_i T_s K_b \left[U(z) - U_r(z) \right] \end{aligned}$$

and by multiplying both sides by z^{-1}:

$$\begin{aligned}(1-z^{-1})U(z) = (1-z^{-1})K_{\mathrm{p}}E(z)\\ + z^{-1}K_{\mathrm{i}}T_{\mathrm{s}}E(z)\\ - z^{-1}K_{\mathrm{i}}T_{\mathrm{s}}K_{\mathrm{b}}\left[U(z)-U_r(z)\right]\end{aligned} \tag{7}$$

Taking the inverse Z-Transforms $Z^{-1}\{U(z)\} = u(k)$, $Z^{-1}\{U_r(z)\} = u_r(k)$ and $Z^{-1}\{E(z)\} = e(k)$, the difference equation becomes:

$$\begin{aligned}u(k)-u(k-1) = K_{\mathrm{p}}(e(k)-e(k-1))\\ + K_{\mathrm{i}}T_{\mathrm{s}}e(k-1) - K_{\mathrm{i}}T_{\mathrm{s}}K_{\mathrm{b}}(u(k-1)\\ - u_r(k-1))\end{aligned}$$

Denoting $u(k)-u(k-1) = \Delta u(k)$ and $e(k)-e(k-1) = \Delta e(k)$, the above equation can be rewritten as:

$$\begin{aligned}\Delta u(k) = K_{\mathrm{p}}\Delta e(k) + K_{\mathrm{i}}T_{\mathrm{s}}e(k-1)\\ - K_{\mathrm{i}}T_{\mathrm{s}}K_{\mathrm{b}}(u(k-1)-u_r(k-1))\end{aligned}$$

During the steady-state behavior of the jet engine, the power delivered by the turbine, W_{t}, equals the power demanded by the compressor, W_{c}. In such situation, there is no variation in rotation speed or in the fuel flow supplied to the engine's combustion chamber. Therefore, for steady-state behavior, the actuation signal sent to the fuel pump, u_r, shall not vary in time, implying that $u_r(k) = u_r(k-1)$. And with no change in rotation speed reference and no rotation speed variation, there must be no variation with time in the PI error, implying that $\Delta e(k) = 0$. The following equation can then be used to describe the behavior of the signal u calculated by the PI for a stable steady-state behavior:

$$\Delta u(k) = K_{\mathrm{i}}T_{\mathrm{s}}e(k-1) - K_{\mathrm{i}}T_{\mathrm{s}}K_{\mathrm{b}}(u(k-1)-u_r(k-1))$$

Using the Z-Transform on the above equation:

$$\begin{aligned}(1-z^{-1})U(z) = z^{-1}K_{\mathrm{i}}T_{\mathrm{s}}E(z)\\ - z^{-1}K_{\mathrm{i}}T_{\mathrm{s}}K_{\mathrm{b}}\left[U(z)-U_r(z)\right]\end{aligned}$$

Resulting in:

$$\begin{aligned}U(z) = \frac{K_{\mathrm{i}}T_{\mathrm{s}}z^{-1}}{1-(1-K_{\mathrm{i}}T_{\mathrm{s}}K_{\mathrm{b}})\,z^{-1}}E(z)\\ + \frac{K_{\mathrm{i}}T_{\mathrm{s}}K_{\mathrm{b}}z^{-1}}{1-(1-K_{\mathrm{i}}T_{\mathrm{s}}K_{\mathrm{b}})\,z^{-1}}U_r(z)\end{aligned} \tag{8}$$

Equation (8) can be rewritten as:

$$\begin{aligned}U(z) = \frac{K_{\mathrm{i}}T_{\mathrm{s}}}{z-(1-K_{\mathrm{i}}T_{\mathrm{s}}K_{\mathrm{b}})}E(z)\\ + \frac{K_{\mathrm{i}}T_{\mathrm{s}}K_{\mathrm{b}}}{z-(1-K_{\mathrm{i}}T_{\mathrm{s}}K_{\mathrm{b}})}U_r(z)\end{aligned} \tag{9}$$

It can be seen from Eq. (9) that, in the case of steady behavior of the engine, $U(z)$ can be described by the sum of two first order transfer functions having the same pole at $1-K_{\mathrm{i}}T_{\mathrm{s}}K_{\mathrm{b}}$ and no zeros. For the obtained discrete transfer functions to be stable, the pole must lie within the unitary circle, leading to the condition $|1-K_{\mathrm{i}}T_{\mathrm{s}}K_{\mathrm{b}}| < 1$. Also, a negative pole will lead to an oscillatory behavior of $U(z)$, which may be undesired and can be avoided if the inequality $1-K_{\mathrm{i}}T_{\mathrm{s}}K_{\mathrm{b}} > 0$ is satisfied. Therefore:

$$1-K_{\mathrm{i}}T_{\mathrm{s}}K_{\mathrm{b}} > 0 \Rightarrow K_{\mathrm{i}}T_{\mathrm{s}}K_{\mathrm{b}} < 1$$
$$1-K_{\mathrm{i}}T_{\mathrm{s}}K_{\mathrm{b}} < 1 \Rightarrow K_{\mathrm{i}}T_{\mathrm{s}}K_{\mathrm{b}} > 0$$

Which leads to design condition:

$$0 < K_{\mathrm{b}} < \frac{1}{K_{\mathrm{i}}T_{\mathrm{s}}} \tag{10}$$

In the particular case, $U_r(z)$ and $E(z)$ are step functions with final values u_{rss} and e_{ss}, respectively, and Eq. (9) can be rewritten as follows:

$$\begin{aligned}U(z) = \frac{K_{\mathrm{i}}T_{\mathrm{s}}}{z-(1-K_{\mathrm{i}}T_{\mathrm{s}}K_{\mathrm{b}})}\frac{z}{z-1}e_{\mathrm{ss}}\\ + \frac{K_{\mathrm{i}}T_{\mathrm{s}}K_{\mathrm{b}}}{z-(1-K_{\mathrm{i}}T_{\mathrm{s}}K_{\mathrm{b}})}\frac{z}{z-1}u_{\mathrm{rss}}\end{aligned}$$

The "Final Value Theorem" can be used to obtain the steady value u_{ss} (of u),

$$u_{\mathrm{ss}} = \lim_{z\to 1}(z-1)U(z)$$

Therefore:

$$u_{\mathrm{ss}} = u_{\mathrm{rss}} + \frac{e_{\mathrm{ss}}}{K_{\mathrm{b}}} \tag{11}$$

Equation (11) shows that u approaches the steady value u_{ss} as the engine remains operating at a steady-state behavior. For smaller values of K_{b}, the pole approaches the unit circle, reflecting a slower time response of u, as can be seen in Eq. (9). It can also be noticed that, in the case of the power management controller, since the control structure intends to follow the power management reference, $e_{\mathrm{ss}} = 0$ and $u_{\mathrm{ss}} = u_{\mathrm{rss}}$. For the limit controllers, however, in most cases, the steady-state value of the error will not equal zero, since the

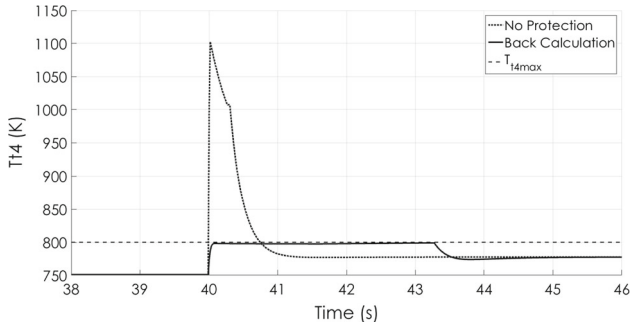

Fig. 7 Response of T_{t4} in for PI structure with no protection and PI structure with Back Calculation applied to T_{t4max} controller

reference used by the limit controllers is not being followed. Therefore, for that case, $u_{ss} = u_{rss} + \frac{e_{ss}}{K_b} \neq u_{rss}$.

To make evident the advantages of applying the Back Calculation anti-windup method, an illustrative hypothetical case is considered where simulations of a Min–Max control system for the GE J85-13 have been accomplished. In this case, besides the main controlled variable N, three other limiters were considered and managed separately in the control structure: maximum acceleration, maximum allowed value of rotation speed, with $N_{max} = 16{,}540$ RPM, and maximum TIT, with $T_{t4max} = 800$ K. PI structures with Back Calculations have been used for the individual compensators, and the main N reference has been changed from 10,000 RPM to 13,000 RPM at the instant 40 s. For this hypothetical case, rotation speed overshoot is admitted as long as N_{max} is not exceeded, a settling time $t_s = 6$ s is considered to be acceptable and T_{t4} must not exceed T_{t4max}.

In a first simulation, the Back Calculation gains $K_{bN} = 10{,}000$ and $K_{bT} = 0$ were adopted, being equivalent to the use of a pure PI structure for the T_{t4} limit controller—which has T_{t4max} as reference value and is responsible for providing temperature protection. Figure 8 shows that control signal coming from the T_{t4} limit controller increases indefinitely and reaches extremely high values, never being selected by the Min logic of the Min–Max structure and, as the rotation speed reference is changed, the T_{t4} limit controller is never activated, as seen in Fig. 10, leading to a high temperature peak value during the engine transient regime which largely exceeds the value of T_{t4max} specified for this hypothetical case, as shown by Fig. 7.

In a second simulation, the Back Calculation gains are set to $K_{bN} = K_{bT} = 10{,}000$. It is shown by Fig. 9 that the control signal coming from the T_{t4} limit controller presents a steady value before the reference is changed, making it suitable for selection by the Min–Max logic. Therefore, when there is a reference change, the T_{t4} limit controller is activated during 4 s, as shown by Fig. 10, and the temperature peak during transient regime does not exceed the desired maximum value of 800 K, as shown in Fig. 7.

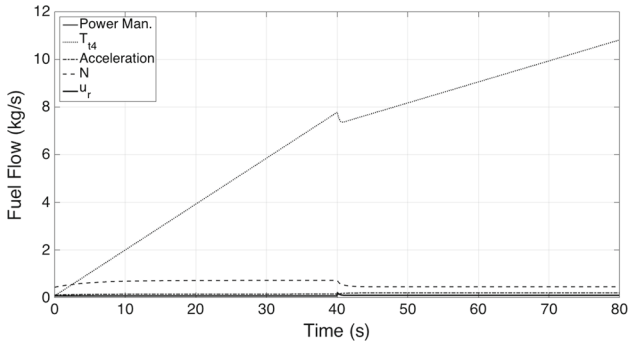

Fig. 8 Actuation signals for PI structure with no protection applied to T_{t4max} controller. In the legend: power man. for power management controller; T_{t4} for T_{t4} limit controller; acceleration for acceleration limit controller; N for N limit controller; u_r for real actuation signal

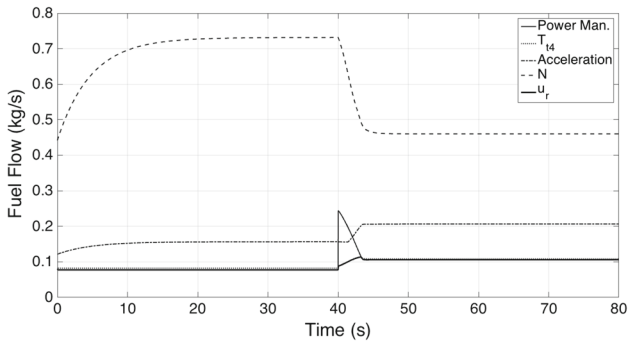

Fig. 9 Actuation signals for PI structure with Back Calculation applied to T_{t4max} controller. In the legend: power man. for power management controller; T_{t4} for T_{t4} limit controller; acceleration for acceleration limit controller; N for N limit controller; u_r for real actuation signal

Figure 11 shows the response of N in both cases, with the rotation speed reference being changed from 10,000 RPM to 13,000 RPM at the instant 40 s. It can be noticed that, although the application of the Back Calculation protection method leads to a slower response with larger overshoot, the specifications established for this hypothetical case concerning N transient regime are still met, with N_{max} not being exceeded and $t_s < 6$ s. Therefore, the application of Back Calculation becomes a better choice over the controller with no protection at all, since Back Calculation protection ensures that the temperature protection becomes active when necessary and that the established value for T_{t4max} is not exceeded, as required.

6 Power Management Controller, Limit Controllers and PI Compensators Design

For the current work, the core rotation speed N has been chosen as the main controlled variable. Therefore, the value for the desired rotation speed is the reference input of the power management controller.

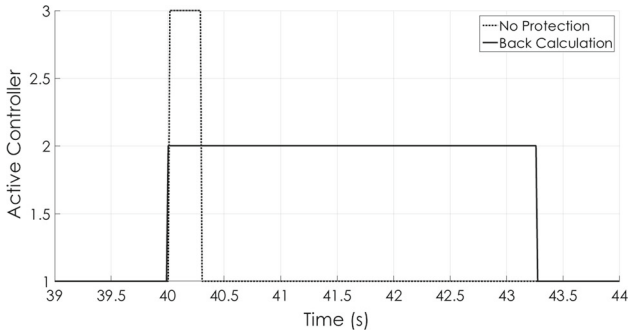

Fig. 10 Active controllers: 2 for T_{t4max} controller; 3 for Max. Accel. controller

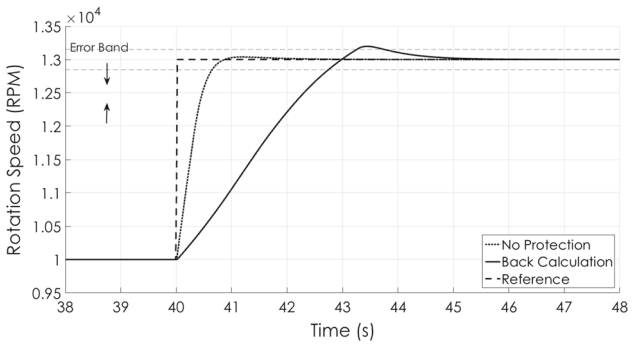

Fig. 11 Rotation speed response for PI structure with no protection and PI structure with Back Calculation applied to T_{t4max} controller

The variables established for the limit controllers are the TIT T_{t4}, which prevents the combustion chamber from achieving excessive temperature levels that could result in turbine thermal damage, the rotation speed N, being used to limit the acceleration in order to avoid compressor stall or surge and to limit the maximum rotation speed allowed in order to avoid mechanical damage. The RU parameter has been chosen to provide an inferior limit used to prevent combustion chamber blow out during deceleration. Therefore, four limit controllers are present in the adopted case study: the N limit controller, preventing the engine to exceed the maximum allowed rotation speed value, the acceleration controller, preventing the engine to operate at regions where there is higher risk of compressor stall, the T_{t4} limit controller, preventing the engine from exceeding the maximum allowed TIT value, T_{t4max}, and the RU limit controller, preventing engine blow out.

For designing the PI compensators, the engine nonlinear model has been linearized around chosen operating points of different steady-state values of N for sea-level, static and standard-day temperature conditions. Also, a linear model has been obtained at the operating points where $T_{t4} = T_{t4max}$, for obtaining the compensator gains used by the T_{t4} limit controller. A cutoff frequency has been chosen at each point where linearization was achieved for designing the corresponding PI compensator and the PI gains have been designed aiming critical dumped closed-loop response or overshoot as low as 2% in case no critical dumping could be achieved at the chosen cutoff frequency.

The current work does not make use of specific linear models for acceleration, differently from what is proposed in Jaw and Mattingly (2009). Therefore, the power management controller, the acceleration limit controller and the N limit controller use the same compensator gains, since they all use the variable N as the controlled variable and have rotation speed values as respective references. Because the complete model is nonlinear and there exist strong dependencies with respect to the operating an ambient conditions, the gain scheduling method is required. Hence, the PI parameters for the power management controller, the acceleration limit controller and the N limit controller are functions of the altitude, flight Mach number and measured value of N. The Back Calculation gain K_{bN} is fixed and does not vary with ambient conditions or measured N value.

The remaining limiters, T_{t4} limit controller and RU limit do not make use of gain scheduling. The T_{t4} limit controller uses fixed gains, and the RU limit controller output is calculated through the multiplication of the measured value of P_{s3} by the established value RU_{min}, not making use of any compensator.

7 Stall Margin Control Through Acceleration Schedule

The choice of a proper value for the stall margin is extremely important in order for proper operation to be guaranteed at all situations. For the current work, the value of 15% was chosen for the stall margin—as defined by the equation below—and must be respected during the transient and the steady-state phases. It is important to mention that the stall margin for the steady-state operating line of the engine is larger then the chosen limit and that the surge avoidance limiter will never keep the engine from reaching any of its steady-state operating points.

$$\mathrm{SM} = \frac{\mathrm{PR_{stall}} - \mathrm{PR}}{\mathrm{PR}} \tag{12}$$

The limitation in acceleration is obtained by the use of a maximum acceleration schedule, being defined as a set of values composed by the maximum step reference values that can be applied to the power management controller that will result in an maximal acceleration that does not violate peak value of 15% for the stall margin. Each entry in the acceleration schedule was obtained for a given value of initial N_c through the simulation of various step values applied to the power management controller until a step value resulted

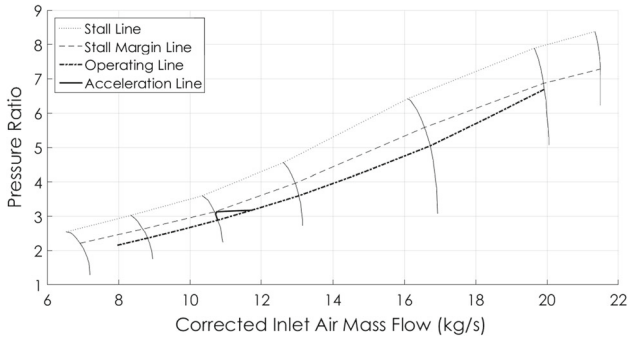

Fig. 12 Step of $N_c = 0.042$ applied to the power management controller

in an acceleration with minimum peak of 15% of stall margin. The simulations have been carried out at sea-level, static and standard-day temperature conditions. For instance, for $N_c = 0.7$, the maximum step value was found to be 0.042 (final value of the step reference $N_c = 0.742$). Such step function, when applied to the power management controller, results in a transient behavior with minimum peak value of 15% of stall margin, as shown by Fig. 12. Tests that have been carried out at different ambient conditions indicate that good conservativeness has been presented by the resulting controller.

The vectors N_c^{Vec} and $\text{AS}_{N_c}^{\text{Vec}}$, described in the following equation, were used in this work. N_c^{Vec} contains the values of N_c where the maximum acceleration value for a minimum stall margin peak of 15% was obtained. $\text{AS}_{N_c}^{\text{Vec}}$ contains the entries for the acceleration schedule, where each entry was obtained through a procedure similar to the one described above for $N_c = 0.7$.

$$\begin{aligned} N_c^{\text{Vec}} &= [0.55\ 0.6\ 0.7\ 0.8\ 0.9\ 0.99] \\ \text{AS}_{N_c}^{\text{Vec}} &= [0.049\ 0.048\ 0.042\ 0.064\ 0.081\ 0.011] \end{aligned} \tag{13}$$

8 Min–Max with Individual Limiter Compensator and Proposed Min–Max with Reference Filter

In general, the Min–Max structure adopts an individual compensator for each limit controller. For comparison proposes, the Min–Max structure has been implemented as shown in Fig. 13, where the power management controller, the acceleration limit controller, the N limit controller, the T_{t4} limit controller and the RU limit controller calculate separate actuation signals to be selected by the Min–Max logic.

The current work proposes an alternative approach with respect to the use of individual compensators for the acceleration limit controller and N limit controller. Instead, the acceleration limitation and the maximum rotation speed limitation are achieved by limiting the allowable maximum reference value of the power management controller at each calculation interaction, i.e., by directly filtering the power management controller reference.

The power management reference filtering is accomplished as follows: First, the instant value of N_c is obtained and the index i is obtained from the vector N_c^{Vec} defined in Eq. (13), where:

$$N_c^{\text{Vec}}(i-1) \leq N_c \leq N_c^{\text{Vec}}(i) \tag{14}$$

A coefficient f is then obtained through the following relation:

$$f = \frac{N_c - N_c^{\text{Vec}}(i-1)}{N_c^{\text{Vec}}(i) - N_c^{\text{Vec}}(i-1)} \tag{15}$$

A maximum variation value for N_c is then calculated from the vector $\text{AS}_{N_c}^{\text{Vec}}$ defined in Eq. (13):

$$\Delta N_c = \text{AS}_{N_c}^{\text{Vec}}(i-1) + f\left(\text{AS}_{N_c}^{\text{Vec}}(i) - \text{AS}_{N_c}^{\text{Vec}}(i-1)\right) \tag{16}$$

The corrected rotation speed N_c is given by the following relation, being N the instant value of the rotation speed:

$$N_c = \frac{N}{N_{\text{D}}\sqrt{\frac{T_{\text{t2}}}{T_{\text{std}}}}} \tag{17}$$

Therefore, the acceleration schedule output value $\text{AS}(N_c)$ can be calculated as follows:

$$\text{AS}(N_c) = (\Delta N_c + N_c)\left(N_{\text{D}}\sqrt{\frac{T_{\text{t2}}}{T_{\text{std}}}}\right) \tag{18}$$

Finally, the calculated output $\text{AS}(N_c)$, the actual desired rotation speed reference, Ref_{N} and the maximum allowed rotation speed, $N_{\max}$, become inputs of a Min block. The Min block's output is the minimum value between $\text{AS}(N_c)$, Ref_{N} and $N_{\max}$, and equals the filtered reference FR_{N}, as defined by the equation below, being adopted as the actual reference for the power management controller. Figure 14 shows the block diagram of the control scheme incorporating the proposed reference filter.

$$\text{FR}_{\text{N}} = \text{Min}(\text{AS}(N_c), N_{\max}, \text{Ref}_{\text{N}}) \tag{19}$$

The reason for proposing such scheme is that, as shown by Eq. (11), the steady value of the calculated actuation signal of any limit controller differs from the steady value of the actual actuation signal sent to the engine's fuel pump. Therefore, in a situation where the engine has been operating at a steady-state operating point for a relatively long time and a sudden

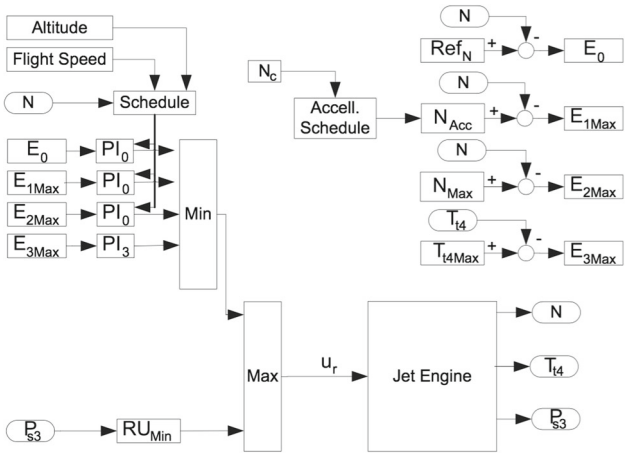

Fig. 13 Classical Min–Max control scheme

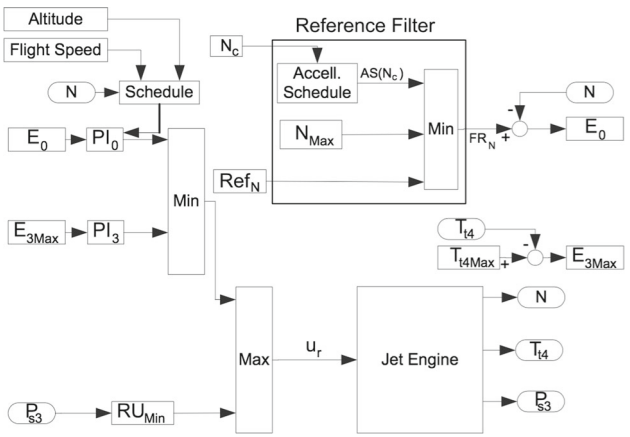

Fig. 14 Min–Max control scheme incorporating the proposed reference filter

acceleration is required, the limit controllers outputs will be initially larger than the power management controller output. The Min–Max structure will therefore select the power management controller output, and the limiters may become inactive for an excessive period of time, causing a more aggressive behavior which may lead to limit exceeding during transient behavior. In the proposed scheme, acceleration and $N_{\max}$ limitations are achieved through sending a smaller reference value whenever needed, therefore avoiding any disputes among any individual limit controllers which use N as a controlled variable or any high output values that would keep them from being selected by the Min–Max logic. Such scheme represents an advantage especially in the case where limiters using other variables then N, such as the T_{t4} limit controller, are activated during very short periods of time, as will be shown in the next section.

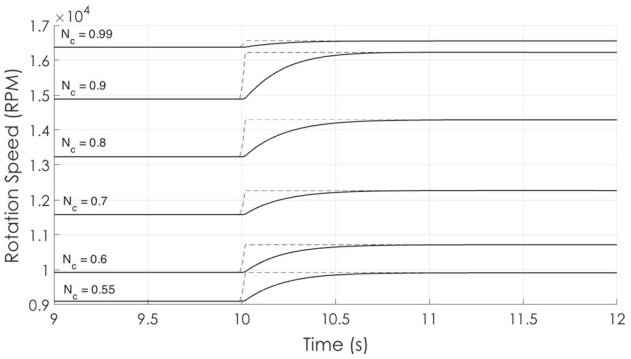

Fig. 15 Maximum N step values for stall margin of 15% applied to each different chosen point of N_c

8.1 Stability Verification

Despite the large use of Min–Max structure with linear compensators in commercial engines, stability analysis of such configuration has only been attempted by few works (Richter 2012b). Johansson (2003) analyzes a similar system with the use of piecewise-linear systems and multiple Lyapunov functions. Overall stability, however, has not been fully considered in the open literature (Richter 2012b).

The proposed method, as well as the method proposed in Csank et al. (2010), utilizes a predefined reference vector for acceleration and maximum variation on speed reference (acceleration schedule) whose values will vary in accordance to the measured core rotation speed N_c. Those proposed schemes add extra nonlinearity to the system, requiring an even more careful analysis in order for a sufficiently rigorous result to be obtained.

This work has verified the closed-loop stability of the Min–Max structure with reference filter by accomplishing numerical simulations at each individual engine operation point of interest, defined by the vector N_c^{Vec} [Eq. (13)]. The step values applied at each point of N_c^{Vec} are defined by vector $\text{AS}_{N_c}^{\text{Vec}}$ [Eq. (13)] in order for a minimum stall margin peak of 15% to be obtained during engine's transient response. The simulation results show that the system is stable in every case, as shown in Fig. 15.

9 Simulation Results

The proposed control scheme was evaluated in a variety of operating conditions. However, for the sake of illustration purposes, a specific operating condition was chosen; namely, at sea-level, standard-day temperature and static conditions, a GE J85-13 remains operating at steady-state regime and $N = 10{,}000$ RPM (minimum thrust condition) for 80 s. At the instant of 80 s, a step is applied to the power management controller demanding the engine to operate at 16,540 RPM

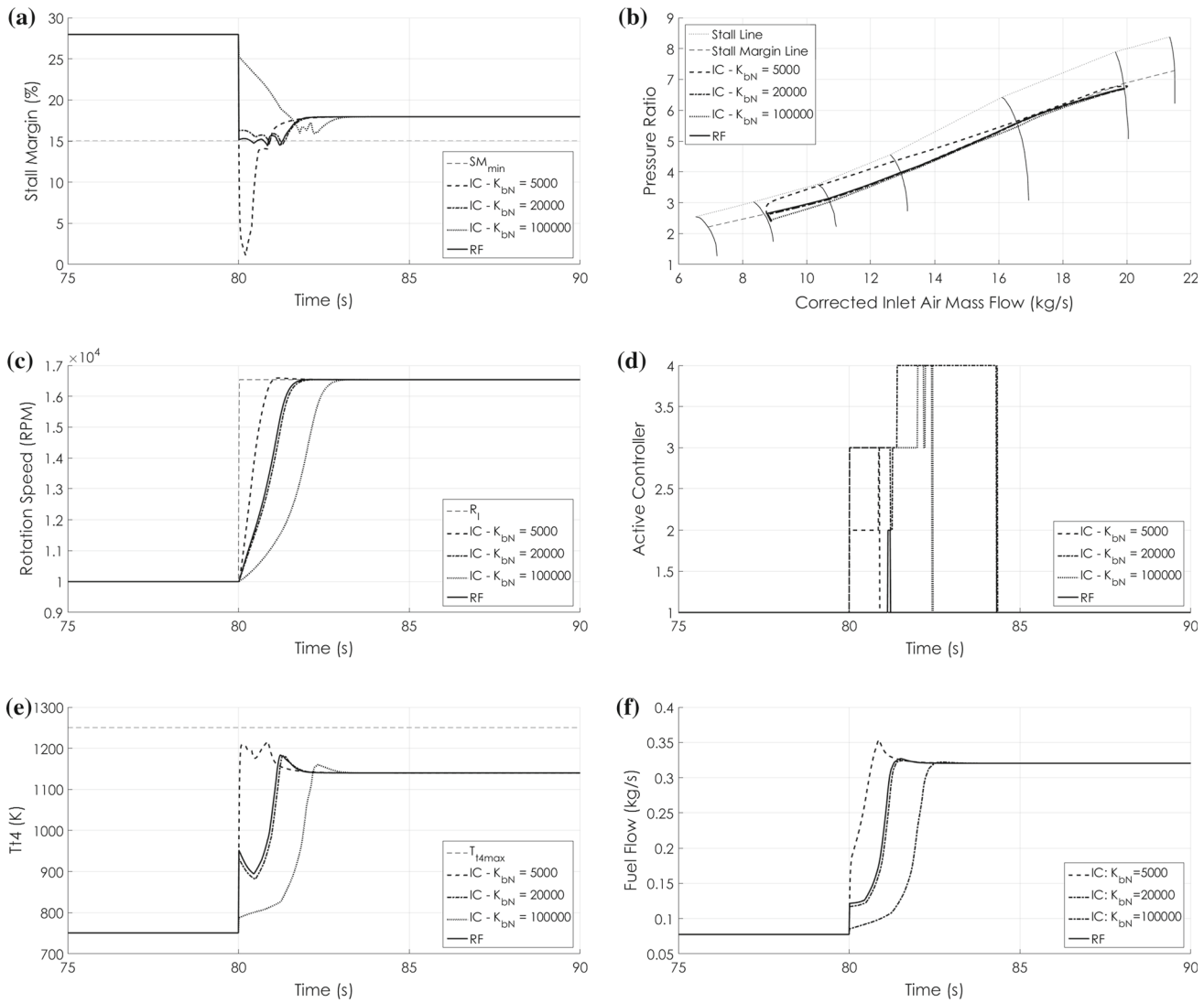

Fig. 16 Simulation results for different values of K_{bN}. **a** Stall margin response for different values of K_{bN}, **b** acceleration lines for different values of K_{bN}, **c** N response for different values of K_{bN}, **d** active controllers for different values of K_{bN}: 1-power management; 2-T_{t4} limiter; 3-acceleration schedule limiter; 4-maximum N limiter, **e** T_{t4} response for different values of K_{bN}, **f** u_r for different values of K_{bN}

(maximum thrust condition), which is the value adopted for N_{max}. For avoidance of high TIT values and combustion chamber blow out, the parameters $T_{t4max} = 1250\,\text{K}$ and $\text{RU}_{min} = 2.8 \times 10^{-7}\,\text{kgm/Ns}$ have been adopted. A settling time of 5 s from minimum thrust condition to maximum thrust condition is considered acceptable in the current evaluation, being this criteria based on the rules established by Federal Aviation Administration (Csank et al. 2010). The above values for rotation speed references and N_{max} have been carefully chosen for the simulation results to remain within the region covered by the real compressor map and the used turbine map, resulting in more reliable results. The values of T_{t4max} and RU_{min} were enough conservative and still did not prejudice the comparison between both control structures.

Simulations have been carried out for, $K_{bN} = 5000$, $K_{bN} = 20{,}000$ and $K_{bN} = 100{,}000$. A constant value $K_{bT} = 10{,}000$ has been adopted and never changed, and all adopted Back Calculation gains meet the condition established by Eq. (10).

The simulation results are shown in Figs. 16 and 17. It can be observed in Fig. 16c that, for the smaller value $K_b = 5000$, the rotation speed N presents a more aggressive behavior, with a relatively low response time ($t_s \approx 1\ s$) when Min–Max with individual compensators is used. However, as shown in Fig. 16a the stall margin did not remain close to the established limit of 15%, presenting a minimum peak of almost 0, which may represent an unsafe situation, since the stall line may be approach the engine static operating line for different reasons, such as steady-state temperature

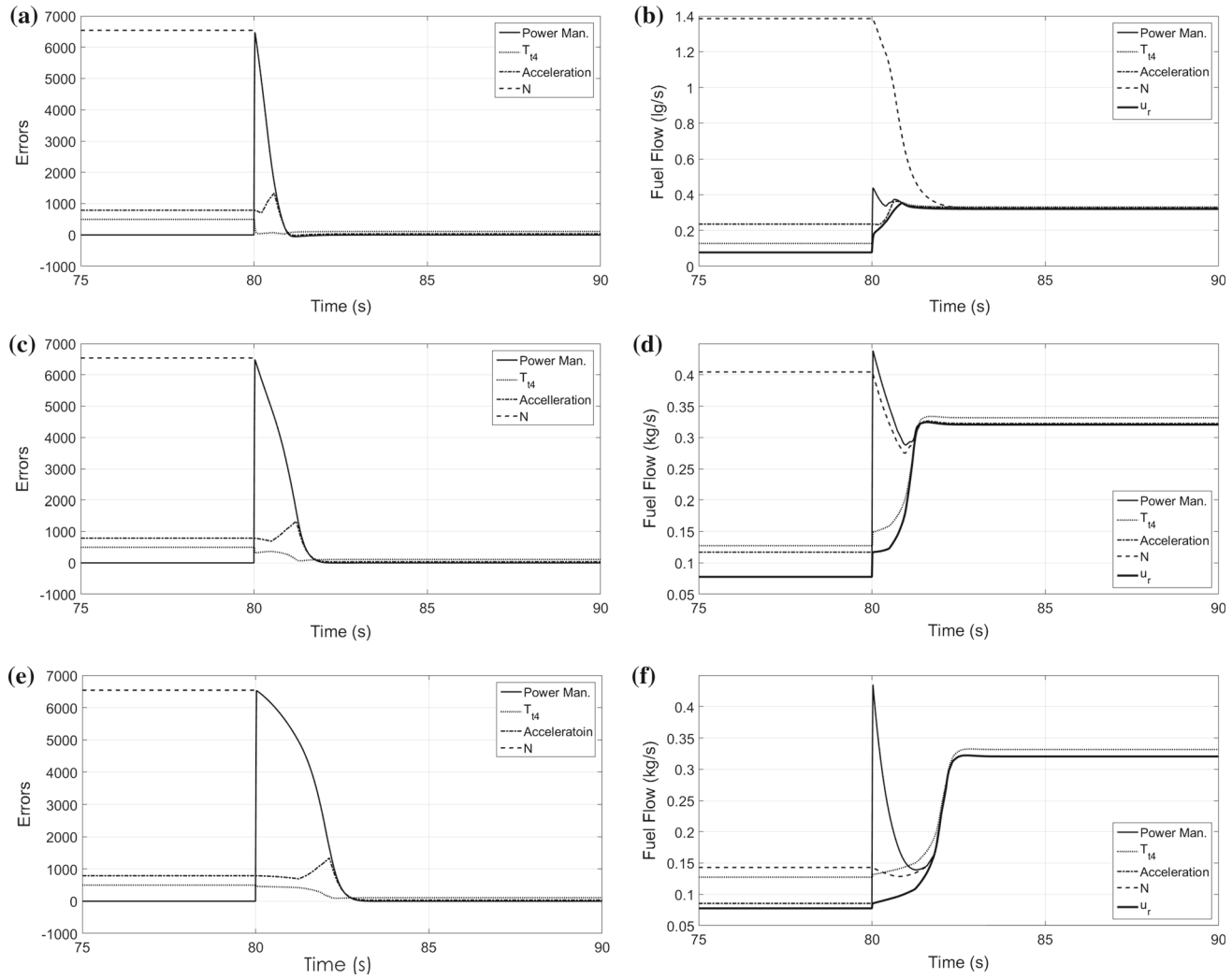

Fig. 17 Errors and w_f for Min–Max with individual compensators. In the legend: power man. for power management controller; T_{t4} for T_{t4} limit controller; acceleration for acceleration limit controller; N for N limit controller; u_r for real actuation signal. **a** $K_b = 5000$, **b** $K_b = 5000$, **c** $K_b = 20{,}000$, **d** $K_b = 20{,}000$, **e** $K_b = 100{,}000$, **f** $K_b = 100{,}000$

and pressure distortions at the compressor inlet (Bobula and Burkardt 1979; Mehalic and Lottig 1974). It can be noticed through the observation of Fig. 16d that the acceleration limit controller is activated for a very short period of time, despite being the one individual limit controller intended to ensure that the stall margin is respected. Instead, the T_{t4} limiter is activated before the acceleration limit controller and remains active for a much longer period. Such behavior can be better understood through the analysis of Figs. 17a, b. The initial steady-state value of the acceleration limit controller output, u_{0as}, and the initial steady-state value of the T_{t4} limit controller, u_{0T}, are obtained with the use of Eq. (11):

$$u_{0as} = u_{0r} + \frac{e_{0as}}{K_{bN}} = 0.0776 + \frac{791}{5000} = 0.236 \text{ kg/s}$$

$$u_{0T_{t4}} = u_{0r} + \frac{e_{0T_{t4}}}{K_{bT}} = 0.0776 + \frac{500}{10{,}000} = 0.128 \text{ kg/s}$$

The initial steady-state value of the power management controller output equals the steady fuel flow value for the initial operation point, i.e., $u_{0pm} = u_{0r} = 0.0776$. It can be noticed that, initially, $u_{0a} > u_{0T_{t4}} > u_{0pm} = u_{0r}$ (Fig. 17b). Because of this initial larger value of u_{0a}, the acceleration limit controller will remain inactive for a period long enough for allowing a more aggressive behavior of the controller and thus prejudicing the stall margin protection. Notice that, due to a higher initial error (Fig. 17a) and the relatively low value of K_{bN}, the initial value of the N limit controller output is much higher then the outputs from the other limit controllers (close to 1.4 kg/s) and this limiter is never activated in this case (Fig. 16d).

When the value of $K_{bN} = 20{,}000$ is used, a lower value of $u_{0a} = 0.117$ kg/s [Eq. (11)] is observed, as shown in Fig. 17d, being much closer to the initial steady value $u_{0r} = 0.0776$ kg/s and lower than $u_{0T_{t4}} = 0.128$ kg/s. This

lower value of u_{0a} allows the acceleration limit controller output to be chosen almost immediately after the reference change, as shown in Fig. 16d, since the power manager controller becomes very aggressive with the reference change (Fig. 17d). However, the value of u_{0a} is still high enough to permit a sufficiently aggressive behavior of the overall controller for a very short period (Fig. 17d), ensuring that the engine operates very close to the established stall margin (Fig. 16a). The rotation speed response, for this case, as observed in Fig. 16c, is 1 s slower that of the previous case, but still acceptable ($t_s \approx 2$ s) and smaller then the established maximum of ($t_s = 5$ s). Notice that, in this case, the T_{t4} limit controller is activated for a very short period of time (Fig. 16d).

For the case of $K_{bN} = 100{,}000$, the initial value $u_{0a} = 0.086$ kg/s is observed, being even closer to the initial value $u_{0r} = 0.0776$ kg/s (Fig. 17f). Again in this case, the acceleration limit controller is activated almost immediately after the reference change (Fig. 16d). This time, however, a lower value of u_{0a} does not allow the controller to remain more aggressive for a period as long as the one in the previous case (Fig. 17f), which results in a slower response of N-over 1 s slower (Fig. 16c), despite still acceptable by the established criteria. The stall margin response, however, is more conservative, with the stall margin remaining larger than the established limit during the entire acceleration regime (Fig. 16a).

It should be noticed that the RU limit controller was never activated, since an acceleration case has been simulated and the rotation speed response was not oscillatory enough to make necessary the activation of this limiter (Fig. 16c). Also, as observed in Fig. 16e, the value of T_{t4} does not exceed the established value of T_{t4max} in any case.

For the cases where the proposed control structure, Min–Max structure with reference filter, has been used, no changes in the controller response were observed regardless of the changes in values of K_{bN}, with the engine response being very similar to the response observed for $K_{bN} = 20{,}000$ and Min–Max structure with individual compensators, as observed in Fig. 16a–f. This independence of K_{bN} may be explained for the fact that, when a reference filter is applied to the power manager controller, the power management controller output will always equal the real actuation signal u_r, since the T_{t4} limit controller remains activate for a very short period (Fig. 16d). The simulation shows that the Min–Max structure with reference filter tends to operate very near the established stall margin (Fig. 16a), since the reference to be sent to the power management controller will be filtered and adapted to any instantaneous protection requirement concerning limitations of rotation speed. The proposed method, therefore, presents the advantage of being simpler to be implemented, requiring only one compensator for implementing the power management controller together with acceleration limit controller and N limit controller (Figs. 13, 14) and also operates closer to the established limits for the limit controllers which use N as controlled variable (Figs. 16, 17), which gives the advantage of a faster and still enough conservative response, when compared to the responses obtained by the Min–Max structure with individual compensators, and higher values of K_{bN}, which are conservative but slower (Fig. 16c).

10 Conclusions

This work proposes a novel approach to design a controller for single-spool jet engines, where the power management controller, the acceleration limit controller and the N limit controller are implemented with the use of a single compensator. The simulation results show that, for the various test cases considered, the new approach yields a better behavior than the scheme with individual compensators, operating closer to the established limit with a sufficiently fast response (in accordance to the established criteria) and suffering lower influence from the K_{bN} gain, which should be carefully set in order for the system not to be too aggressive or too slow. The new approach also presents the advantage of having a simpler implementation, eliminating the need for an individual compensator design for the acceleration limit controller, as proposed in previous work (Jaw and Mattingly 2009; Csank et al. 2010), and using a single compensator to implement the power management controller, the acceleration limit controller and the N limit controller.

Eventual disadvantages have also been observed in the proposed method and must be taken into consideration in more detailed future studies. Robustness and a reduction in the grid of operating points where locally linear models are obtained have not been investigated in this work, where a large grid has been adopted aiming better investigation of the proposed method itself. The use of a more refined grid would require more hardware resources, leading to a more expensive practical implementation. Also, it is noticed that the maximum values of N step are a function of the corrected speed N_c, which can only be calculated if total inlet temperature and pressure are measured. Obtaining the maximum step values from a direct measurement of N would require larger tables and more hardware memory during implementation, since, at different altitudes, the same value of N_c corresponds to a different value of N. Finally, the proposed method introduces an extra nonlinearity to the Min–Max conventional structure, demanding large effort for a formal complete stability analysis to be accomplished. It is important to mention that, even for the conventional Min–Max structure, complex questions such as global stability have not yet been fully considered by literature (Richter 2012b).

Future work might also contemplate the use of the proposed Min–Max structure with reference filter to simplify the control structure of two-axis turbofan jet engines, which is commonly implemented with the use of Min–Max structure with individual compensators. Experimental tests should be also carried out to validate the new approach in single-spool jet engines and turbo fan jet engines.

References

Bobula, G. A., & Burkardt, L. A. (1979). Effects of the steady-state pressure distortion on the stall-margin of a J85-21 turbojet engine. Technical Memorandum NASA TM-79123, NASA, NASA Lewis Research Center, Cleveland, OH 44135, USA. https://ntrs.nasa.gov/?R=19790015797. Accessed 12 Nov 2017.

Chappman, J., et al. (2014). Toolbox for the modeling and analysis of thermodynamic systems (T-MATS) user's guide. Technical Memorandum NASA/TM-2014-216638, NASA, NASA Glenn Research Center, Cleveland, OH 44135, USA. https://ntrs.nasa.gov/search.jsp?R=20140012486. Accessed 27 Apr 2016.

Chapman, J. W., et al. (2016). Practical techniques for modeling gas turbine engine performance. In *52nd AIAA/SAE/ASEE joint propulsion conference, American Institute of Aeronautics and Astronautics*. https://doi.org/10.2514/6.2016-4527.

Chapman, J. W., & Litt, J. S. (2017). Control design for an advanced geared turbofan engine. In *53rd AIAA/SAE/ASEE joint propulsion conference, American Institute of Aeronautics and Astronautics*. https://doi.org/10.2514/6.2017-4820.

Csank, J., et al. (2010). Control design for a generic aircraft engine. In *46th AIAA/SAE/ASEE joint propulsion conference, American Institute of Aeronautics and Astronautics*. https://doi.org/10.2514/6.2010-6629.

Hodel, A. S., & Hall, C. E. (2001). Variable-structure PID control to prevent integrator windup. *IEEE Transactions on Industrial Electronics*, *48*(2), 442–451.

Imani, A., & Montazeri-Gh, M. (2017). Improvement of min–max limit protection in aircraft engine control: An lMI approach. *Aerospace Science and Technology*, *68*, 214–222.

Jaw, L., & Mattingly, J. (2009). *Aircraft engine controls: Design, system analysis and health monitoring. Chap 5–6* (pp. 119–170). Reston: American Institute of Aeronautics and Astronautics.

Johansson, M. (2003). *Piecewise linear control systems* (pp. 57–61). Berlin: Springer.

Kopasakis, G. (2010). Volume dynamics propulsion system modeling for supersonics vehicle research. *ASME Journal of Turbomachinery*, *132*(4), 041003–041003-8. https://doi.org/10.1115/1.3192148.

Mehalic, C. M., & Lottig, R. A. (1974). Steady-state inlet temperature distortion effects on the stall limits of a J85-GE-13 turbojet engine. Technical Memorandum NASA TMX-2990, NASA Lewis Research Center, Cleveland, OH 44135, USA. https://ntrs.nasa.gov/search.jsp?R=19740009394. Accessed 12 Nov 2017.

Richter, H. (2012a). *Advanced control of turbofan engines, chap 1* (pp. 1–4). New York: Springer.

Richter, H. (2012b). Multiple sliding modes with override logic: Limit management in aircraft engine controls. *Journal of Guidance, Control and Dynamics*, *35*(4), 1132–1142.

Visioli, A. (2003). Modified anti-windup scheme for PID controllers. *IEEE Proceedings: Control Theory and Applications*, *150*(1), 49–54.

Yarlagadda, S. (2010). Performance analysis of J85 turbojet engine matching thrust with reduced inlet pressure to the compressor. Master of science degree dissertation, The University of Toledo, Toledo, Spain.